Vibronic photoexcitation spectra of irradiated spinel MgO· nAl_2O_3(n=2) at low temperatures

Abu Zayed Mohammad Saliqur Rahman[a,*], Xingzhong Cao[a], Long Wei[a], Baoyi Wang[a], Shuaishuai Sun[b], Ye Tao[b], Qiu Xu[c]

[a] *Key Laboratory of Nuclear Analytical Techniques, Institute of High Energy Physics, Chinese Academy of Sciences 19B Yuquanlu Shijingshan District Beijing 100049, China*
[b] *Beijing Synchrotron Radiation Facilities, Institute of High Energy Physics, Chinese Academy of Sciences 19B Yuquanlu Shijingshan District Beijing 100049, China*
[c] *Reactor Research Institute, Kyoto University 2, Asashiro-Nishi, Kumatori-cho, Sennan-gun, Osaka 590-0494, Japan*

chinaXiv:201703.00563v1

Abstract

A vibronic photoexcitation band at approximately 230 nm was found at 13 K in reactor neutron- and electron-irradiated magnesium aluminate spinel (MgO·$n$$Al_2O_3$). Vibronic structure was found to be temperature dependent and became obscure at over 120 K. Huang Rhys factor S and Debye Temperature Θ_D were estimated from the temperature dependence of the 230 nm band by curve-fitting method using Debye approximation. Origin of the vibronic photoexcitation band was suggested as F center.

Keywords: vibronic structure, irradiation, F center, vacancy, MgO·$n$$Al_2O_3$

1. Introduction

Magnesium aluminate spinel (MgO·$n$$Al_2O_3$) is an oxide with tolerance to irradiation. This material is a good candidate for some important applications in advanced fusion reactor technology such as window materials for radio frequency heating, insulating materials and liquid metal cooling system[1, 2, 3]. The crystal structure of the MgO·$n$$Al_2O_3$ consists of a cubic cell with $Fd3m$ symmetry, containing a close-packed array of 32 oxygen atoms with cations in tetrahedral and octahedral interstices[4]. Relatively complex structure comparing to those of its constituent oxides MgO and α-Al_2O_3 makes the study of defect more difficult. Formation of both anion (F-type center) and cation (V-type center) vacancies is possible by neutron irradiation in spinel single crystals. Studies of irradiation induced point defects such as F- type centers in MgO·$n$$Al_2O_3$ were reported for both stoichiometric and non-stoichiometric spinel crystals[4, 5, 6, 7, 8]. F-center absorption band shifts towards higher energies in non-stoichiometric spinel crystals because of lattice constant. This shift in absorption band is consistent with Mollvo-Ivey relation[6]. Vibronic F type centers at low temperatures were reported for MgO[9] and α-Al_2O_3[10, 11]. However, there is no report on the vibronic photoexcitation (PE) band in MgO·$n$$Al_2O_3$($n$=2) to the best of our knowledge. F-center excitation band in neutron-irradiated non-stoichiometric spinel has tail at higher energy region which falls below 6.2 eV or 200 nm. To measure the excitation spectra in the vacuum ultraviolet (VUV) range we have used synchrotron radiation light source.

In the present study, we used VUV spectroscopy to investigate the anion vacancies in neutron- and electron-irradiated MgO·$n$$Al_2O_3$ single crystals. Vibronic F-center PE spectra of irradiated magnesium aluminate spinel were reported for the first time. Temperature dependent feature of the vibronic excitation band provided the information to estimate Huang-Rhys factor (electron-phonon coupling constant) and Debye temperature.

2. Experimental

Single crystals of undoped non-stoichiometric magnesium aluminate spinel (MgO·$n$$Al_2O_3$) ($n$ = 2) grown by Czochralski method were provided by Furuuchi Chemical Co., Japan. The typical size of the samples was $7 \times 5 \times 1$ mm^3. The samples were irradiated with reactor neutrons and electrons at low temperatures. Neutron bombardment was performed by using low-temperature loop (LTL) facility in Kyoto University Reactor Research Institute (KURRI) at 20 K. Total irradiation dose was 1.3×10^{17} n/cm^2, which corresponds to 6.9×10^{-5} displacement per atom (dpa) estimated by using the average displacement energy 52 eV [12]. Electron-irradiation was performed at liquid nitrogen temperature by using electron linear accelerator (KURRI-LINAC). The energy of electron beam was 30 MeV with fluence of 5.8×10^{18} e/cm^2 at a flux of 1.6×10^{14} e/cm^2·sec.

Photoluminescence (PL) spectra were measured using the VUV beamline 4B8 of the Beijing Synchrotron Radiation Facility (BSRF) in Institute of High Energy Physics (IHEP), Chinese Academy of Sciences (CAS). The electron energy of the storage ring was 2.5 GeV and the beam current was approximately 240 to 160 mA in measurement. PE and PL spectra

*Corresponding author
Email addresses: zayed82000@yahoo.com (Abu Zayed Mohammad Saliqur Rahman), caoxzh@ihep.ac.cn (Xingzhong Cao), weil@ihep.ac.cn (Long Wei)

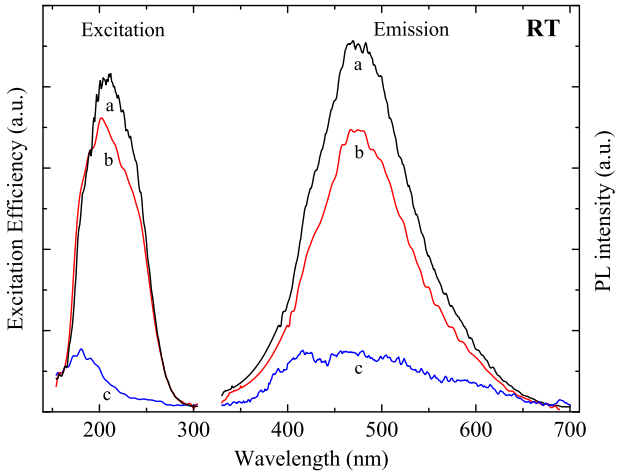

Figure 1: (Color online)VUV-UV photoexcitation (left) and photoluminescence (right) spectra of irradiated and unirradiated $MgO{\cdot}nAl_2O_3$ (n = 2). Electron- (a), neutron-irradiated (b) and unirradiated (c) samples. Observation wavelength: 476 nm. Excitation wavelength: 219 nm.

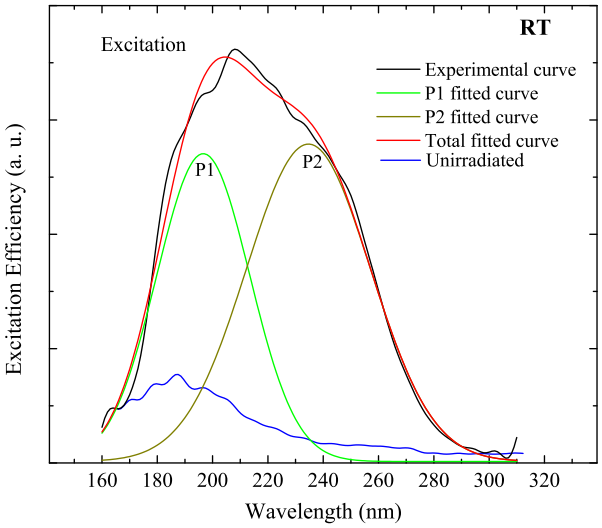

Figure 2: (Color online) Photoexcitation spectra of neutron-irradiated and unirradiated spinel samples at room temperature. Observation wavelength: 476 nm.

were measured at temperatures 13 to 290 K. PE spectra were measured at wavelengths 125 to 350 nm and PL spectra were measured at wavelengths 330 to 700 nm. Seya-Namioka type grating monochromator (1200 L/mm) was used for measuring PE spectra and ACTON SP308 monochromator (1200 L/mm) was used to measure PL spectra. The spectral resolution of the system is 0.2 nm. The signal was detected by a Hamamatsu H8259-01 photon counting head. PE spectra were calibrated by using sodium salicylate signal.

3. Results

3.1. VUV-UV photoexcitation spectra

Figure 1 shows the VUV-UV PE (left) and PL (right) spectra of irradiated and unirradiated spinel samples at room temperature. Emission spectra were measured under the 219 nm. PE spectra were obtained by monitoring luminescence at 476 nm. Peak position of the PE band was found at approximately 210 nm in electron- and neutron-irradiated samples whereas the peak positions for the unirradiated sample found at approximately 190 nm. Emission peak was found at approximately 475 nm for electron- and neutron-irradiated samples. Unirradiated sample shows no obvious peak on the emission band. The emission peak at approximately 475 nm band shifted to 465 nm at low temperatures in electron- and neutron-irradiated samples (Fig. 3).

Figure 2 shows the extended PE spectrum of neutron-irradiated sample with full-width half-maximum (FWHM) of about 77 nm. The spectrum was fitted by Gaussian curve fitting. P1 (green dash) and P2 (green) show the Gaussian curves calculated by fit multi-peaks method using OriginPro-8 program. Peak positions of the P1 and P2 bands were estimated to be 195 and 235 nm, respectively. The experimental curve (black line) is fitted well with the total fit (red line). PE spectrum of unirradiated sample (blue line) was represented for comparison.

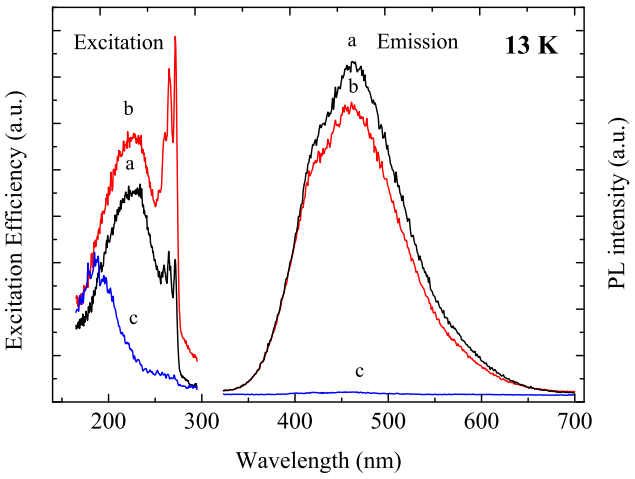

Figure 3: (Color online) Vibronic photoexcitation (left) and emission spectra of electron- (a), neutron-irradiated (b) and (c) unirradiated spinel samples at 13 K. Observation wavelength : 380 nm. Excitation wavelength: 240 nm.

3.2. Vibronic photoexcitation spectra

Figure 3 (left) shows the vibronic PE spectra of electron- (a), neutron-irradiated (b) and unirradiated (c) spinel samples obtained by monitoring luminescence at 380 nm. These spectra were measured at 13 K. Vibronic features appeared due to weak electron-phonon coupling at low temperatures. Peak position of the vibronic excitation band was at approximately 230 nm. Peak positions of the vibronic lines and the energy separations are listed in Table 1. Unirradiated sample shows no vibronic PE band. Emission spectra of electron- (a), neutron-irradiated (b) and unirradiated (c) spinel samples were also shown in Fig. 3 (right).

Figure 4 shows the vibronic PE spectra of neutron-irradiated spinel monitored at various wavelengths on 465 nm emission band (Fig. 3). Intensity of the most intense line at 271.3 was higher than the broad excitation band when monitored at 380

chinaXiv:201703.00563v1

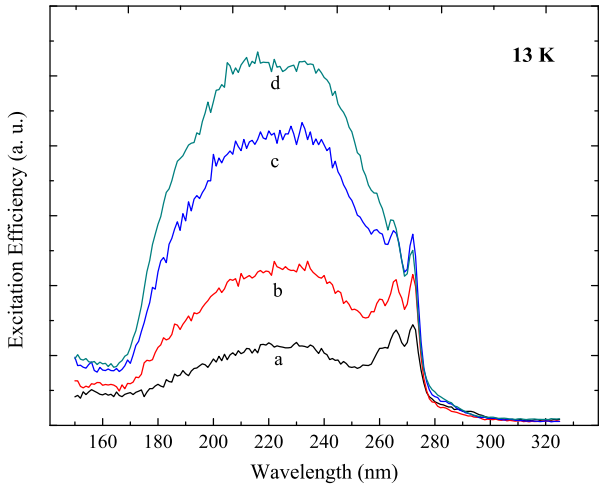

Figure 4: (Color online) Vibronic photoexcitation spectra of neutron-irradiated spinel at 13 K, monitored at (a) 380 (b) 400 (c) 430 and (d) 465 nm.

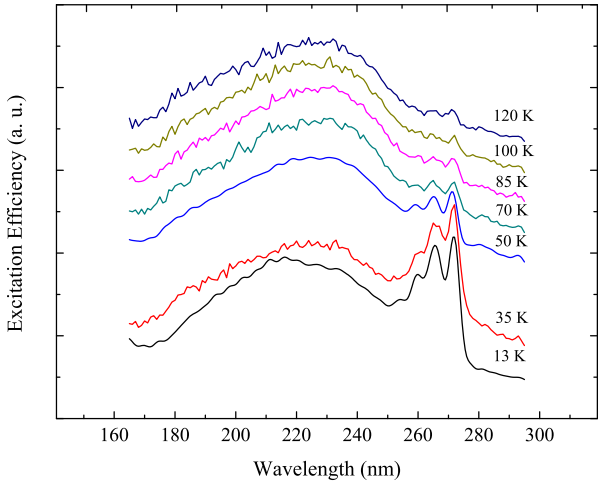

Figure 5: (Color online) Vibronic photoexcitation spectra of neutron-irradiated sample at temperatures 13 to 120 K. Observation wavelength:380 nm.

nm. Intensity of the main broad band approximately at 230 nm gradually increased when monitored at longer wavelengths than 380 nm.

3.3. Temperature dependence

Figure 5 shows the vibronic PE spectra of neutron-irradiated sample at temperatures 13 to 120 K. Intensity of the sharp lines decreased with increasing temperature and becomes obscure at over 120 K.

Figure 6 shows the estimation of Debye temperature Θ_D and Huang-Rhys factor S from temperature dependence of the 230 nm (5.39 eV) vibronic PE band by using Debye approximation [11]. Intensity ratio of the sharp line to broad band is represented by the following equation in Debye approximation. Equation 1 works well when measuring temperature $T << \Theta_D$.

$$\frac{I_s}{I_b} = \exp[-S\{1 + \frac{2\pi^2}{3} \times (\frac{T}{\Theta_D})^2\}] \quad (1)$$

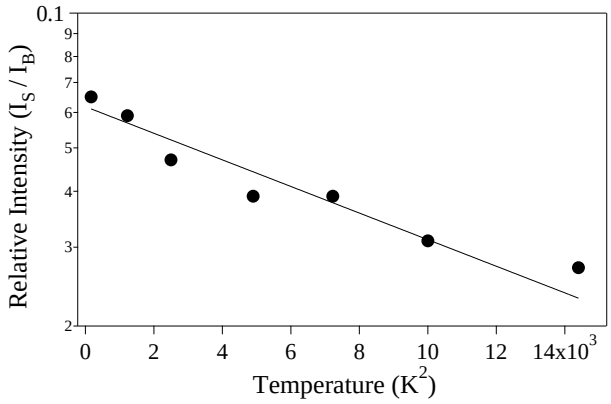

Figure 6: Estimation of Debye temperature and Huang Rhys factor S from temperature dependence of the 230 nm vibronic photoexcitation band (Fig. 4) by curve fitting method.

In Eqn. (1), I_s and I_b are the integrated intensities of the prominent sharp line and the broad excitation band, respectively. Huang-Rhys factor was estimated to be $S = 2.78$ and the Debye temperature to be $\Theta_D = 518$ K by curve fitting Fig. 6 with Eqn. (1).

4. Discussion

Figure 1 shows the excitation and emission spectra of the neutron-, electron-irradiated and unirradiated samples. Emission band at approximately 475 nm (2.6 eV) was tentatively assigned to F center (two electrons trapped in an oxygen vacancy) [5]. This band shifted to 465 nm at low temperatures (Fig. 3). LTL facility was used to induce simple defects such as F-type centers in the materials[13]. In Fig. 2, overlapping bands P1 and P2 were estimated by Gaussian multi peak curve fitting. The P1 band at approximately 195 nm was also found in unirradiated sample. Thus, this peak may be due to presence of Fe^{3+} impurity[6, 7]. The P2 band at approximately 235 nm, which was not observed in unirradiated sample, is due to irradiation-induced defect and assigned to F-center excitation[7]. The intensity of the F-center excitation band increased significantly and shifted towards higher energy at low temperatures.

Figure 3 shows the vibronic F-center excitation band and emission band after exposure to neutron and electron irradiation at 13 K. Vibronic PE spectra was observed for the first time. This vibronic structure was only observed at low temperatures and becomes obscure at over 120 K (Fig. 5). The vibronic structure was well observed monitoring the luminescence at 380 nm in shorter wavelength region of the 465 nm emission band (Fig. 4). To assign the zero-phonon line (ZPL), observation of the vibronic emission spectra with most intense line at 271.3 line is expected but experimental observation of the defect-related vibronic excitation and emission spectra is not always easy. Nevertheless, the prominent sharp line at 271.3 nm may be tentatively assigned to ZPL and other lines at 264.8, 260.5 and 254.0 nm assigned to phonon assisted lines, as energy separations between the sharp lines are approximately spaced

chinaXiv:201703.00563v1

Table 1: Sharp lines associated with 230 nm photoexcitation band, estimated Huang-Rhys factor and Debye temperature.

Band (Excitation)	Line number	Wavelength (nm)	Wavenumber (cm^{-1})	Photon energy (eV)	Energy Separation (cm^{-1})	Huang-Rhys Factor	Debye temperature (K)
	0	271.3	36860	4.58	0		
230 nm	1	264.8	37764	4.69	904	2.78	518
	2	260.5	38388	4.77	624		
	3	254.0	39370	4.89	982		

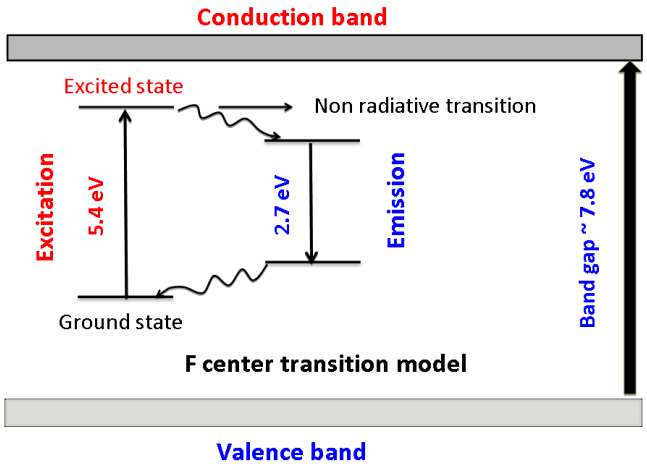

Figure 7: (Color online) Schematic diagram of F-center transition in irradiated MgO· nAl$_2$O$_3$ (n = 2).

regularly. Phonon frequencies at 624, 904 and 982 cm^{-1} were not in agreement with calculation of the phonon spectrum of $MgAl_2O_4$ spinel[14] which suggested that the phonon modes active in this transition are localized and caused by radiation damage.

Huang-Rhys factor S=2.78 estimated from Fig. 6 is small enough to observe vibronic structure. Debye temperature Θ_D=518 K was found smaller than that (Θ_D=803 K) of the powdered spinel[15] . Characteristic Debye frequency of the spinel crystal may be different from that of the defect-related localized F centers. Therefore, the low Debye temperature may be due to the localized centers caused by atomic displacement defects. Defect-related Debye temperature decreased in both MgO[16] and α-Al_2O_3[11, 17] comparing to that of normal modes.

Figure 7 represents the schematic diagram of the excitation and emission process which took place within the band gap (7.8 eV) of the $MgAl_2O_4$[18] . After absorbing the energy of the 5.4 eV (230 nm), F center is excited from the ground state to a higher energy excited state and relaxed to the ground state after emitting phonon and photon with energy 2.7 eV (465 nm).

5. Conclusion

In this study, vibronic PE spectra in neutron- and electron-irradiated MgO· nAl$_2$O$_3$(n=2) was detected for the first time by VUV-UV spectroscopic measurement. This vibronic band was assigned to F center. Physical parameters such as Debye temperature and Huang-Rhys factor were estimated from the temperature dependence of the vibronic excitation band.

Acknowledgment

We would like to thank the staffs of KURRI for their technical support during irradiation of the samples. We are gratefully acknowledged to Dr. K. Atobe for fruitful discussion. This work was partially supported by the NSFC (Grant Nos.91026006 and 10835006) and Chinese Academy of Sciences Fellowships for Young International Scientists under Grant No. 2012Y1JB0007.

References

[1] A. Turos, Hj. Matzke, A. Drigo, A. Sambo, and R. Falcone, Nucl. Instrum. Methods Phys. Res. B 113 (1996) 261.
[2] C. G. Lee, T. Ohmura, Y. Takeda, S. Matsuoka, and N. Kishimoto, J. Nucl. Mater. 326 (2004) 211.
[3] Nan Jiang, and John C. H. Spence, J. Nucl. Mater. 403 (2010) 147.
[4] V. T. Gritsyna, I. V. Afanasyev-Charkin, V. A. Kobyakov, and K. E. Sickafus, J. Am. Ceram. Soc. 82 (1999) 3365.
[5] P. K. Bandyopadhyay, and G. P. Summers, Phys. Rev. B 31 (1985) 2422.
[6] V. T. Gritsyna, I. V. Afanasyev-Charkin, Yu. G. Kazarinov, and K. E. Sickafus, Nucl. Instrum. Methods Phys. Res. B 218 (2004) 264.
[7] G. P. Summers, G. S. White, K. H. Lee, and J. H. Crawford, Phys. Rev. B 21 (1980) 2578.
[8] V. T. Gritsyna, and Yu. G. Kazarinov, Nucl. Instrum. Methods Phys. Res. B 250 (2006) 349.
[9] M. Nakagawa, and K. Ozawa, J. Phys. Soc. Japan, 24 (1968) 96.
[10] L. S. Welch, A. E. Hughes, and G. P. Pells, J. Phys. C: Solid St. Phys. 13 (1980) 1805.
[11] R. A. Z. M. Saliqur, T. Awata, N. Yamashita, Qiu Xu, and K. Atobe, Radiat Eff. Def. Solids 164 (2009) 692.
[12] Z. He, and P. Jung, Nucl. Intstrum. Methods Phys. Res. B 166-167 (2000) 165.
[13] M. Okada, S. Kanazawa, T. Nozaki, M. Nakagawa, K. Atobe, E. Kuramoto, K. Matsumura, and T. Sano, Nucl. Instrum. Methods Phys. Res. A 463 (2001) 213.
[14] G. A. de Wijs, C. M. Fang, G. Kresse, and G. de With, Phys. Rev. B 65 (2002) 094305-1.
[15] M. J. Iqbal, and B. Ismail, J. Alloys Compd. 472 (2009) 434.
[16] Y. Kazumata, K. Ozawa, and M. Nakagawa, Phys. Lett. 19 (1965) 529.
[17] R. A. Z. M. Saliqur, T. Awata, N. Yamashita, Y. Inada, K. Oshima, Q. Xu, and K. Atobe, Physics Procedia 2 (2009) 551.
[18] M. L. Bortz, R. H. French, D. J. Jones, R. V. Kasowski, and F. S. Ohuchi, Physica Scripta 41 (1990) 537.

chinaXiv:201703.00563v1